



- Molecular evidence on potential contribution of
- 2 marine emissions to aromatic and aliphatic
- 3 organic sulfur and nitrogen aerosols in the
- 4 South China Sea
- 6 Yu Xu^{1,2}, Yi-Jia Ma^{1,2}, Ting Yang^{1,2}, Qi-Bin Sun^{3,4}, Yu-Chen Wang,⁵ Lin Gui^{1,2}, Hong-
- 7 Wei Xiao^{1,2}, Hao Xiao^{1,2}, Hua-Yun Xiao^{1,2}*
- ¹School of Agriculture and Biology, Shanghai Jiao Tong University, Shanghai 200240,
- 10 China

- 11 ²Shanghai Yangtze River Delta Eco-Environmental Change and Management
- 12 Observation and Research Station, Ministry of Science and Technology, Ministry of
- 13 Education, Shanghai 200240, China
- ³Dongguan Meteorological Bureau, Dongguan, Guangdong, 523086, China
- ⁴Dongguan Engineering Technology Research Center of Urban Eco-Environmental
- 16 Meteorology, GBA Academy of Meteorological Research, Dongguan, Guangdong,
- 17 523086, China
- ⁵College of Environmental Science and Engineering, Hunan University, Changsha,
- 19 Hunan, 410082, China
- 20 *Corresponding authors
- 21 Hua-Yun Xiao
- E-mail: xiaohuayun@sjtu.edu.cn
- 23 Phone: +86-173-0183-7060





24 Abstract: The origins of marine aromatic and aliphatic secondary organic aerosols (SOA) remain elusive. Here, organosulfates (OSs) and nitrogen-containing organic 25 compounds (NOCs) were measured in PM2.5 collected in Sansha (the South China 26 Sea), a region with minimal anthropogenic pollution, to investigate the potential 27 28 impact of marine emissions on their formation. The proportion of aliphatic and aromatic OSs in the total OSs was significantly higher in Sansha than in other Chinese 29 30 cities investigated. Biogenic OSs correlated significantly with aliphatic and aromatic 31 OSs and NOCs. Two typical SOA tracers (C₆H₅O₄S⁻ and C₇H₇O₄S⁻), which are 32 formed via the atmospheric oxidation of marine benzene and toluene, were found to 33 increase with rising chlorophyll-a and isoprene levels in seawater. Additionally, the impact of long-range transport and ship emissions on the abundance of OSs and 34 35 NOCs was found to be insignificant. These results together with mantel test analysis suggest that marine-derived precursors may significantly contribute to the formation 36 of aliphatic and aromatic OSs and NOCs in the Sansha region. Overall, this study 37 provides the observation-based molecular evidence that marine biogenic emissions 38 39 may play a significant role in the formation of aromatic and aliphatic SOA in the South China Sea. 40

41

42 **Keywords:** Aerosol particles, Organosulfates, Nitrogen-containing organic

43 compounds, Marine emissions, Aliphatics and aromatics

44

45

48





1. Introduction

environments and climate systems, influencing air quality, climate, elemental 49 biogeochemical cycle, and human health (Takeuchi et al., 2022; Jimenez et al., 2009; 50 51 Huang et al., 2014). While much of the previous research has primarily focused on terrestrial SOA, there has been an increasing interest in marine-derived SOA in the 52 53 past decade due to their potential influence on cloud formation and radiative forcing 54 over marine areas (Lawler et al., 2020; Wang et al., 2023; Wohl et al., 2023; Hansen et 55 al., 2014; Yu and Li, 2021; Meskhidze and Nenes, 2006). Understanding the occurrence, origins, and formation of marine SOA is essential for accurately assessing 56 their climatic and environmental impacts. The identification of SOA molecular 57 58 markers is a fruitful approach to investigate the origins and formation processes of 59 marine SOA (Wang et al., 2023). These markers function as chemical fingerprints, enabling researchers to trace precursors and elucidate transformation pathways 60 (Bushrod et al., 2024; Yang et al., 2024; Jaoui et al., 2019; Ma et al., 2025). 61 62 Although anthropogenic inputs transported from coastal and inland regions can contribute to the marine SOA (Zhou et al., 2023), volatile organic compounds (VOCs) 63 emitted by phytoplankton and other marine biota are the primary origins of marine 64 native SOA (Zhao et al., 2023; Hu et al., 2013). It has been documented that the 65 oxidation of biogenic isoprene, monoterpenes, and dimethyl sulfide in the marine 66 boundary layer promotes the formation of SOA markers, such as organosulfates (OSs), 67 nitrooxy OSs, and oxygenated hydrocarbons (Hu et al., 2013; Wang et al., 2023; 68

Secondary organic aerosols (SOA) play a critical role in atmospheric





Hansen et al., 2014; Moore et al., 2024). As indicated by a recent observational study, 69 70 marine biogenic emissions of benzene and toluene have the potential to contribute to 71 the formation of SOA in the oceanic environment, though direct aerosol molecular evidence for this is currently lacking (Wohl et al., 2023). Benzene and toluene are 72 73 traditionally associated with anthropogenic combustion sources (Cabrera-Perez et al., 74 2016). These compounds have been detected in the air of temperate oceans and 75 remote polar areas (Colomb et al., 2009; Wohl et al., 2023), indicating their 76 widespread distribution as organic species in the marine atmosphere. Indeed, marine 77 phytoplankton and other marine biota also have the capability of releasing various 78 aliphatic and aromatic VOCs (Yu and Li, 2021; Weisskopf et al., 2021). However, the lower abundance of marine aliphatic and aromatic VOCs compared to isoprene and 79 80 monoterpenes makes their detection challenging, potentially resulting in their 81 oversight in atmospheric models and research endeavors (Yu and Li, 2021; Zhao et al., 2023). Specifically, aliphatic- and aromatic-derived SOA markers (e.g., aliphatic and 82 aromatic OSs) are rarely identified in marine atmospheric observation research 83 84 (mainly focusing on isoprene- and monoterpenes-derived SOA) (Wang et al., 2023). Consequently, our present understanding of the role of marine-derived aliphatic and 85 aromatic VOCs in the formation of organic aerosols remains limited. 86 Extant research on marine biogenic SOA (BSOA) has been concentrated on 87 88 temperate and polar regions (Hawkins et al., 2010; Wozniak et al., 2014; Lawler et al., 2020; Wang et al., 2023; Bushrod et al., 2024), with relatively limited attention given 89 to the tropics, where environmental conditions differ significantly. The South China 90





91 Sea, with tropical climate, is one of the most biologically productive marine regions 92 (Zhai et al., 2018), positioning it as an optimal location to study the marine BSOA 93 components. Here, we presented the quantification of 92 OSs and measurements of nitrogen-containing organic compounds (NOCs) and other chemical components in 94 95 PM_{2.5} collected in the Sansha region (South China Sea) over a one-year period. This study aims to elucidate the potential origins and formation of tropical marine aerosol 96 97 OSs and NOCs, with a focus on the impacts of marine organism emissions on the 98 formation of aromatic and aliphatic organic aerosols. The findings of this work were 99 expected to not only provide crucial molecular evidence for marine-derived aromatic 100 and aliphatic SOA markers but also help to deepen our understanding of the ocean-101 atmosphere interaction.

102

103

104

105

106

107

108

109

110

111

112

2. Materials and methods

2.1. Study site description and sample collection

The Sansha area, situated in the South China Sea, is located more than 410 kilometers from Hainan Island. This area has a tropical maritime climate, which is characterized by high average temperatures (27°C) and relative humidity (84%) throughout the year (**Table S1**). The favorable climate of the Sansha region is conducive to its rich biodiversity and complex ocean ecosystems. Aerosol sampling was conducted from August 23, 2017 to August 28, 2018 on the roof (~15 m above the ground) of the Xisha Deep Sea Marine Environment Observation and Research Station, South China Sea Institute of Oceanology (Chinese Academy of Sciences)

114

115

116

117

118

119

120

121

122

123

124

125

126

127

128

129





(Figure S1) in the Sansha area. For a considerable duration, Sansha has functioned as a pivotal nexus of geopolitical tensions in the South China Sea (Carrico, 2020; Ming, 2016). Consequently, the region has been in a closed or semi-closed state, particularly during the period of the 2018 US-China trade dispute. Without considering the impact of long-range transport of pollutants, the unique geographical characteristics of Sansha resulted in a considerable small anthropogenic pollution in the local area during the sampling campaign. PM_{2.5} samples were collected at a steady flow rate $(1.05 \pm 0.03 \text{ m}^3 \text{ min}^{-1})$ on prebaked (500 °C for 10 h) quartz fiber filters (Pallflex, Pall Corporation, USA) using a high-volume air sampler (KC-1000, Laoying, China). The collection period for each PM_{2.5} sample was approximately 72 h to ensure that the enriched SOA markers could be determined. A blank sample was collected on a monthly basis. A total of 71 samples were collected and stored at -30 °C (S1 in Supporting Information). The data of relative humidity (RH), temperature (T), and the concentrations of nitrogen oxides (NO_x) and ozone (O₃) during the sampling campaign were obtained from the adjacent monitoring stations. These data will be averaged based on the collection time of each PM_{2.5} sample.

130

131

132

133

134

2.2. Measurements and data analysis

The procedures for extraction, identification, and quantification of OSs have been described in detail in our recent studies (Yang et al., 2024; Yang et al., 2023).

Briefly, the samples were extracted with methanol, followed by filtration using a 0.22

135

136

137

138

139

140

141

142

143

144

145

146

147

148

149

150

151

152

153

154

155





µm Teflon syringe filter (CNW Technologies GmbH). Thereafter, the solution was concentrated under a gentle stream of nitrogen gas. Finally, the extracts mixed with 300 μ L Milli-Q water (~18.2 M Ω cm) were used for analysis (Acquity UPLC-MS/MS; Waters, USA). The processing of the mass spectrometry data was conducted using the MassLynx v4.1 software, which facilitated the acquisition of information pertaining to m/z, formula, and signal intensity. The identification of 33 types of OS compounds has been validated through the confirmation of sulfur-containing fragment ions (e.g., m/z 80, 81, and 96) by MS/MS analysis (Yang et al., 2023; Wang et al., 2021). More details regarding the identification, classification, and quantification of OSs and relevant limitations were described in S2 in Supporting Information. A total of up to 155 OSs were identified, of which 92 OSs were quantified using the surrogate standards. All OSs were undetectable in the blank samples. The recoveries of the surrogate standards ranged from 84% to 94% (S2 in Supporting Information). It should be noted that the potential impacts of sampling without removal reactive gases (e.g., SO₂ and NO_x) for OS and NOC (introduced below) analysis were not considered, as indicated by many previous studies (Yang et al., 2024; Wang et al., 2023; Jaoui et al., 2019; Huang et al., 2014). This is because if SO2 and NOx can react with compounds on filters to generate SOA, analogous reaction processes can also take place on ambient particles prior to sampling. Indeed, no study has been conducted to systematically evaluate the relative efficiency of SOA formation in ambient particles and filters.





156 The extraction procedure of NOCs was similar to that of OSs. NOCs were also analyzed using Acquity UPLC-MS/MS system. However, NOC identification (i.e., 157 CHON-, CHON+, and CHN+ compounds) was conducted in both electrospray 158 ionization positive (ESI+) and negative (ESI-) ion modes. The detailed extraction and 159 160 analysis methodologies for NOCs have been well documented in our recent publications (Ma et al., 2024; Ma et al., 2025) and S2 in Supporting Information. 161 162 Given the inherent uncertainties associated with ionization efficiencies across diverse 163 compounds and the utilization of different measuring instruments (Ditto et al., 2022), 164 an intercomparison of the relative abundance of compounds identified with the same 165 analytical approach and instrument by the same person was performed in the present study (Ma et al., 2025). This can maximize the consistency of analysis and the 166 167 reliability of the results. Furthermore, we classified the OS groups as follows (details in S2 in 168 Supporting Information): isoprene-derived OSs (OSi), monoterpenes-derived OSs 169 (OS_m), aliphatic- and aromatic-derived OSs (they were collectively referred to as 170 171 OSa), and OSs with two or three carbon atoms (i.e., C2-C3 OSs) (Tables S2-S3). The system identification of potential precursors of NOCs was conducted by synthesizing 172 the methodology delineated in previous studies (Nie et al., 2022; Guo et al., 2022; Ma 173 174 et al., 2025) (S3 in Supporting Information). The categorization of CHON- and 175 CHON+ compounds was refined into the following subgroups, including isoprene-, 176 monoterpenes-, aromatic-, and aliphatic-derived oxidized-NOCs (Ox-NOCs) and aliphatic-, and heterocyclic-derived reduced-NOCs (Re-NOCs). 177 aromatic-,





178 Additionally, CHN+ compounds were categorized into monoaromatic, polyaromatic, 179 and aliphatic subgroups. A comprehensive account of the modified workflow for the classification of NOCs based on potential precursors was furnished in Figure S2 and 180 S2 in Supporting Information. 181 182 For the analysis of inorganic ions, an additional portion of each filter sample was extracted with Milli-Q water using an ultrasonic bath (~4 °C). The extracts were 183 184 subsequently filtered through a PTFE syringe filter. Inorganic ions including SO₄²⁻, NH₄⁺, K⁺, NO₃⁻, Mg²⁺, Ca²⁺, Na⁺, and Cl⁻ were quantified using an ion 185 186 chromatograph system (Dionex Aquion, Thermo Scientific, USA) (Yang et al., 2025; 187 Xu et al., 2019; Xu et al., 2022). The pH value was predicted with a thermodynamic model (ISORROPIA-II) (Xu et al., 2020b; Xu et al., 2023; Yang et al., 2024) (details 188 189 in S4 in Supporting Information). The sea surface temperature (SST) data (0.25°× 190 0.25°) were derived from NOAA Optimum Interpolation Sea Surface Temperature Version 2 (OISSTv2) dataset. Chlorophyll-a (Chl a) concentration data (0.5°×0.5°) 191 192 were derived from the MODIS Level-3 product processed with the OC5 algorithm 193 and acquired from the GlobColour. To prevent the extraction of missing values, the 194 nearest available values within the radius of 0.75° and 1° around the sampling location were averaged and assigned. Isoprene concentrations in surface seawater were 195 196 predicted by an empirical formulas that depends on temperature and Chl a (i.e., 197 20.9[Chl a]-1.92[SST]+63.1) (Wang et al., 2023). Notably, although uncertainties may 198 exist in predictions of seawater-surface isoprene, the predicted trend in its concentration changes was expected to be reliable. The gridded VOC emissions from 199





200 international shipping (0.1°×0.1°) were extracted from the HTAPv3 mosaic emission inventory (Crippa et al., 2023; Huang et al., 2017). To characterize the long-range 201 202 transport pathways of air masses arriving at the sampling site during each sampling event, 3-day (72 h) back trajectories beginning at 500 m above sea level were 203 204 computed using TrajStat v1.5.4 implemented in MeteoInfoMap 3.3.0 (Chinese Academy of Meteorological Sciences, China). The data used for trajectory calculation 205 206 were obtained from NOAA's Air Resources Laboratory 207 (ftp://arlftp.arlhq.noaa.gov/pub/archives/gdas1/). The fire data were derived from 208 NASA's Fire Information for Resource Management System 209 (https://firms.modaps.eosdis.nasa.gov/active fire/). The concentrations of non-sea-salt (nss) potassium ion was calculated by subtracting 0.022 times the sodium ion 210 211 concentration from the total potassium ion concentration (Chen et al., 2010).

212

213

214

3. Results and discussion

3.1. Compositions and abundances of OSs and NOCs

215 **Figure 1a** compares the average concentrations of OS_i , OS_m , C_2 - C_3 OS_8 , and OS_a in Sansha with those observed in other regions worldwide. OS_i was the most abundant aerosol OS subgroup in Sansha, averaging 12 ± 3 ng m⁻³ and contributing $32 \pm 3\%$ to the total OSs. The second most abundant OS subgroup was C_2 - C_3 OSs (30 \pm 4%), followed by OS_a (23 \pm 2%) and OS_m (16 \pm 2%). The total OS concentrations in Sansha ranged from 26 to 93 ng m⁻³, exhibiting an average of 39 \pm 13 ng m⁻³. A global summary of the observation data suggested that the highest mean OS





concentration (2157 ng m⁻³) was recorded at a forest park site in Look Rock, TN, USA (Budisulistiorini et al., 2015) and the lower level (generally less than 2 ng m⁻³) was observed in both urban and polar sites (Hansen et al., 2014; Ma et al., 2014). The observed OS concentrations in this study fell within the range of values previously documented (**Table S4**). Generally, the predominance of OS_i in the total OSs has been extensively reported in various observations conducted in different regions, including Xi'an, China (Yang et al., 2025), Guangzhou, China (Bryant et al., 2021; Yang et al., 2025), Beijing, China (Yang et al., 2025), Shanghai, China (Yang et al., 2023), the Yellow Sea, China, Patra, Greece (Kanellopoulos et al., 2022), Towson, MD, USA (Meade et al., 2016), and the Amazon forest (Riva et al., 2019) (**Table S4**). A plausible explanation for these observations is the presence of a substantial biogenic emission of isoprene.

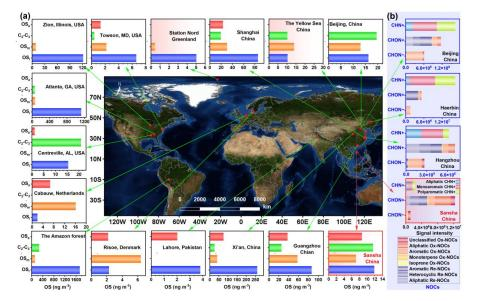


Figure 1. A comparison of (a) the concentrations of isoprene-derived OSs (OSi),





237 monoterpenes-derived OSs (OS_m), C₂-C₃ OSs, and aliphatic- and aromatic--derived 238 OSs (OS_a) in PM_{2.5} in Sansha and other regions worldwide (more data in **Table S4**). (b) Average signal intensity distributions for the CHON+, CHN+, and CHON-239 compounds from various sources in PM_{2.5} collected in Sansha and other Chinese cities. 240 241 The NOC data were identified using the identical analysis methodology (Ma et al., 242 2025). In addition, it is important to acknowledge that not all OS species have been 243 detected in all locations, and the absence of OSs in some panels does not necessarily 244 imply their nonexistence. The figure may contain a territory that is disputed according to the United Nations.

246

247

248

249

250

251

252

253

254

255

256

257

258

245

A notable finding of this study was that the proportion of OSa in the total OSs in Sansha Island (23%, on average) was higher than the observed results in most other cities (Figure 1a and Table S4). In order to minimize potential discrepancies stemming from different measurement methods and the types of OS detected, we conducted a comparison of our previous OS data, measured in different regions of China, with the data obtained from Sansha (Yang et al., 2023; Yang et al., 2025). These data were evaluated using the identical analysis methodology. Indeed, the mass fractions of OS_a in the total OSs in Xi'an (inland; 19%), Guangzhou (coastal; 18%), and Shanghai (coastal; 12%) were smaller than that in Sansha Island, although the OSa concentration was lower in Sansha Island (Figure 1a and Table S4). The attribution of this phenomenon to the long-range transport of pollutants from coastal cities in China may not be a reasonable assumption. This is due to the fact that the

260

261

262

263

264

265

266

267

268

269

270

271

272

273

274

275

276

277

278

279

280





transmission effect was incapable of inducing an increase in the proportion of OSa from coastal cities with developed industries (e.g., Shanghai and Guangzhou) to Sansha Island (see section 3.3 for further evidence). Despite the absence of quantitative research on the aliphatic and aromatic OSs in the marine aerosols previously, the relatively high proportion of OSa in the Sansha region compared to industrialized inland and coastal cities in China suggested either marine phytoplankton (/microorganisms) or ships had released large amounts of aliphatic and aromatic precursors to promote the formation of OS_a locally. Figure 1b presents the average signal intensity distributions of different NOCs from various precursors in Sansha, inland (Beijing and Haerbin; urban site) (Ma et al., 2025), and coastal (Hangzhou; urban site) (Ma et al., 2025) areas of China. It is noteworthy that the data presented herein employed the same measurement and data analysis methods by the same person. On average, aromatic-derived Ox-NOCs accounted for 12% of the total signal intensity of CHON- compounds in Sansha, which was significantly lower than the observations (72%–90%) recorded in Beijing, Haerbin, and Hangzhou. However, the mean signal intensity proportion of identified isoprene- and monoterpenes-derived Ox-NOCs in the total signal intensity of CHONcompounds was much higher in Sansha (29%) than in Beijing, Haerbin, and Hangzhou (2%–3%). The mean atmospheric NO₂ level in the Sansha area (**Table S1**) was found to be more than 10 times lower than that observed in inland urban areas (Ma et al., 2025), which may significantly constrain the formation of aromatic-derived

Ox-NOCs. However, the total release of isoprene and monoterpenes from marine





281 sources in the Sansha area may account for a higher proportion of the total NOC 282 precursors than aromatic compounds, likely causing the proportion of isoprene- and monoterpenes-derived Ox-NOCs to be relatively higher than that of aromatics-derived 283 284 Ox-NOCs. 285 The mean signal intensity proportion of aromatic-derived CHON+ type Re-NOCs in the total signal intensity of CHON+ compounds was also lower in Sansha 286 287 (30%) than in Beijing (48%), Haerbin (88%), and Hangzhou (35%). The reaction of 288 carbonyl compounds with NH₄⁺ (or NH₃) in the aqueous phase has been suggested to 289 form Re-NOCs (Gen et al., 2018). Thus, the significantly lower (over 10 times) levels 290 of aerosol NH₄⁺ in Sansha (**Table S1**) relative to other cities (Ma et al., 2025) may be one of the important factors constraining Re-NOC formation. In addition, the signal 291 292 intensity fraction of aromatic-derived CHN+ type Re-NOCs in the total signal 293 intensity of CHN+ compounds was lower in Sansha (28%) than in inland urban pollution areas (37%-41%; Beijing and Haerbin) but higher than in the coastal area 294 (14%; Hangzhou). Overall, sulfate and atmospheric oxidation capacity would not be a 295 296 constraint for OS formation, owing to the abundant source of marine sulfate and the 297 strong solar radiation in the tropical ocean (Sansha) (Xiao et al., 2017). However, the presence of low local NO_x and NH₄⁺ levels may impose constraints on the formation 298 of aerosol NOCs in the Sansha area. However, the observation of high OSa mass 299 300 fractions and aromatic-derived Re-NOC peak intensity fractions (Figure 1) in Sansha at least suggests that the composition of organic aerosols in this region is significantly 301 influenced by aliphatic and aromatic precursors. The subsequent results will provide 302





further evidence to support this consideration.

304

305

307

308

309

310

311

312

313

314

315

316

317

318

319

320

321

322

323

324

303

3.2. Temporal variations of SOA marker groups and implications for their

306 origins

Figures 2a,b show the temporal variations in the concentrations of the various OS subgroups. The mass concentrations of OSi, OSm, and OSa tended to increase from autumn (Aug – Nov) to winter (Dec – Feb), with the maximum value in February. Subsequent to February, there was a gradual decrease in the concentrations of various OSs, and the fluctuations in their concentrations over time stabilized. It should be noted that this tropical sea area does not exhibit a distinct seasonal pattern, attributable to the small air temperature variation between summer and winter (Table S1). Additionally, the SST value was lowest in February ($24 \pm 1^{\circ}$ C) (Figure S3a and Figure S4), corresponding to the highest levels of isoprene in surface seawater (Figure S3b). The isoprene concentration in surface seawater underwent a decrease and subsequent stabilization after April, exhibiting a resemblance to the temporal patterns observed in various OSs. The variation patterns among SST, seawater isoprene levels, and Chlorophyll-a obtained from empirical formulas or satellite data presented here are consistent with actual observation results in the South China Sea (Zhai et al., 2018). It is therefore evident that the parameters applied here (e.g., seawater isoprene levels and Chlorophyll-a) function as reliable indicators. These findings suggest that the formation of these OSs, at least for well-defined biogenic VOCs-derived OSs (e.g., OSi and OSm), may be closely related to marine

326

327

328

329

330

331

332

333

334

335

336

337

338

339

340

341

342

343

344

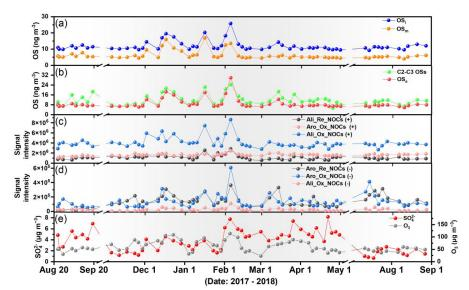




phytoplankton emissions.

Sulfate and particle acidity have been suggested to be the important factors controlling the formation of OSs (Yang et al., 2023; Surratt et al., 2008; Brüggemann et al., 2020). Due to the high sulfate level and low ammonium level in PM2.5 in the Sansha area, the investigated aerosol particles are all acidic (Table S2). This is very favorable for aerosol OS formation. The aerosol sulfate concentration in the Sansha area was also higher than our observed value in Shanghai, while the various OS concentrations were found to be lower than those in Shanghai (the same OS measurement method and identification type) (Yang et al., 2023). Furthermore, insignificant correlations (P > 0.05) were found between sulfates and OS_i , OS_m , C2-C3 OSs, and OSa, as expected from the dissimilar temporal patterns for these variables (Figures 2a,b,e). Interestingly, these OSs showed significant correlations (r > 0.6, P < 0.01) with local O₃ levels. The above results suggest that aerosol OSs in the Sansha area may be mainly formed locally and are tightly associated with precursor emission levels (e.g., abovementioned phytoplankton emissions) rather than sulfates. Aerosol OSa is generally regarded as anthropogenic-derived OSs in inland urban areas (Yang et al., 2024; Yang et al., 2025). Previous studies have suggested that marine phytoplankton and other marine biota are capable of releasing aliphatic and aromatic VOCs (Yu and Li, 2021; Weisskopf et al., 2021). Thus, the above findings may also imply that aromatic and aliphatic precursors emitted by marine organisms are potential sources of aerosol OSa in the Sansha area.





identified in ESI- mode, respectively.

Figure 2. Temporal variations in (a, b) the concentration of the different OSs, (c-f) the signal intensity of the various CHON+, CHN+, and CHON- compounds from different sources, and (f) the concentration of sulfate and ozone. Ali_Re_NOCs (+), Aro_Ox_NOCs (+), and Ali_Ox_NOCs (+) refer to the aliphatic-derived reduced form NOCs, aromatic-derived oxidized form NOCs, and aliphatic-derived oxidized form NOCs identified in ESI+ mode, respectively. Aro_Re_NOCs (-), Aro_Ox_NOCs (-), and Ali_Ox_NOCs (-) refer to the aromatic-derived reduced form NOCs, aromatic-derived oxidized form NOCs, and aliphatic-derived oxidized form NOCs

Figures 2c,d show the temporal variations in the signal intensities of the various aromatic- and aliphatic-derived NOCs. These aromatic- and aliphatic-derived NOCs identified in ESI+ mode showed an overall consistent temporal trend, a pattern of which was highly similar to that of OS_i and OS_m (r up to 0.82, P < 0.01). Moreover,





the aromatic- and aliphatic-derived NOCs detected in ESI+ mode were significantly (0.55 < r < 0.66, P < 0.01) positively correlated with O_3 and O_x $(O_3 + NO_2)$. In contrast, the aromatic- and aliphatic-derived NOCs detected in ESI- mode showed a relatively weak positive correlation (0.36 < r < 0.49) with O_3 and O_x . OS_i and OS_m were two typical types of biogenic OSs (Yang et al., 2023; Wang et al., 2023; Surratt et al., 2008). Thus, the overall results not only suggest that the formation of OS_a was related to marine biogenic sources (as discussed above), but also imply that the formation of aromatic and aliphatic NOCs (at least for those detected in ESI+ mode) may be influenced by biogenic sources. The subsequent discussion will present additional evidence regarding the contribution of aromatic and aliphatic precursors released from the ocean to the formation of aerosol sulfur-containing and nitrogen-containing organic compounds.

3.3. Insignificant impact of long-range transport and ship emissions

The long-range transport of pollutants from coastal areas or marine traffic (i.e., ship) emissions has been suggested to be an important contributor to the inorganic and organic components of marine aerosols (Zhou et al., 2023; Wang et al., 2023). Specifically, a previous study in the Sansha area during the years 2014–2015 suggested that the inorganic components in aerosols may be influenced by biomass burning-related pollutants transported from the northeast and southwest directions of Sansha (Xiao et al., 2017). In order to examine the potential roles of long-range transport and ship emissions in the formation of aerosol OSs and NOCs in the Sansha

384

385

386

387

388

389

390

391

392

393

394

395

396

397

398

399

400

401

402

403





area, variations in the air mass transmission patterns (Figure 3a), nss-K⁺ abundances (Figure 3b), and ship emissions of non-methane VOCs were investigated (Figure 4). Cluster analysis of air mass backward trajectories indicated that air masses arriving at the sampling site primarily originated from the northeast sea area during the winter and spring months (December - May). This period coincided with heightened biomass burning activity in the southwest coastal regions (Figure 3). Conversely, during other periods, biomass burning activity exhibited a marked decline, with air masses predominantly originating from the southwestern and northeastern sea areas. Nevertheless, the concentrations of nss-K⁺, used as a typical biomass burning tracer (Liang et al., 2021), demonstrated no variability in accordance with the direction of the air masses or the intensity of biomass burning in coastal areas. For example, a relatively stable level of nss-K+ was observed during the specified period (December - May), which corresponded to the period of maximum biomass burning intensity. The high nss-K⁺ event occurred in August 2018, which can be attributed to 94% of the air masses passing through coastal areas where biomass burning occurred. However, the OS concentrations did not increase during that month. In particular, the Sansha area belongs to the tropical ocean with high ultraviolet radiation, making it almost impossible for VOCs such as isoprene and gaseous reactive nitrogen to be transported here from the nearest coast more than 410 kilometers away. These results indicate that long-range transport exerted a weak impact on organic aerosol composition in the Sansha area.

405





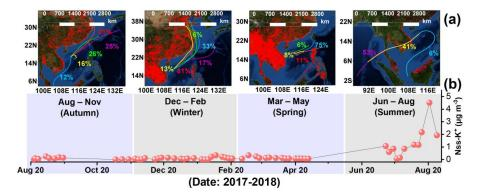


Figure 3. Air mass back trajectories (72 h; 500 m above ground level) and fire spots

408 (NASA active fire data, VIIRS 375 m) during different periods, with corresponding

409 temporal variations in (b) the concentration of nss-K⁺. The map in panel (a) was

derived from MeteoInfoMap (Chinese Academy of Meteorological Sciences, China).

Figures 4a,b show the temporal variation in the amount of the total non-methane VOCs (NMVOCs; with the exception of isoprene and monoterpenes) and major VOCs emitted from ships in the Sansha area. The emission levels of NMVOCs, isoprene, and monoterpenes were lowest in February–March (Figure 4b and Figure S5), which was opposite to the temporal variation patterns of various OSs and aromatic- and aliphatic-derived NOCs (Figure 2). In other months, the level of NMVOCs from ship emissions remained relatively stable. This can be attributed to the unique geographical location of the Sansha area, where the government exercises stringent control over the number of passable ships in the surrounding sea areas. Thus, the above results suggest that ship emissions were not the primary factor in controlling the abundance of aerosol OSs and NOCs in the Sansha area. These findings, combined with the previously mentioned fact that OSa proportion was higher





in Sansha than in China's industrialized inland and coastal cities, further demonstrate that the ocean can release aliphatic and aromatic precursors to facilitate in situ OS_a formation.

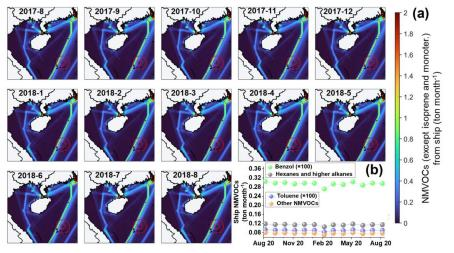


Figure 4 Illustrations presenting (a) the variation in the amount of non-methane VOCs (NMVOCs; with the exception of isoprene and monoterpenes) emitted from ships over months in the Sansha area. (b) Temporal variations in the emission amount of several important NMVOCs. The small and large red circles in panel b show radii of 0.25° and 0.75°, respectively.

3.4. Potential impact of marine biological emissions to aromatic and aliphatic organic sulfur and nitrogen aerosols

According to the aforementioned analysis, we can propose that the aerosol OSs and aromatic- and aliphatic-derived NOCs in the Sansha area may be locally formed and closely related to the marine biological emissions. A Mantel test correlation





analysis was conducted to further investigate the impact of different factors on the formation of OSs and NOCs in the Sansha area (Figure 5). We found that the abundances of OS_i, OS_m, and OS_a were significantly related to various impacting factors, including Na⁺, RH, O₃, O_x, Chl a, and SST. Sodium ions and Chl a have been identified as important indicators of marine sources (Wang et al., 2023; Xiao et al., 2017). Ozone and its photolysis related products (major source of ·OH in the ocean atmosphere) are important oxidants for OS formation (Yang et al., 2023). The RH of the air in the Sansha area is consistently high throughout the year (84%, Table S1), which plays a significant role in the liquid phase formation of OSs (Yang et al., 2024). Thus, these results support our previous consideration that ocean emissions not only control the formation of OS_i and OS_m, but also significantly affect the formation of aliphatic- and aromatic-derived OSs. The principal component analysis result showed a high aggregation effect of Na⁺, O₃, O_x, Chl a with various OSs (Figure 6a), further indicating that the emissions of marine phytoplankton promoted the local formation of aerosol OS in the Sansha area.





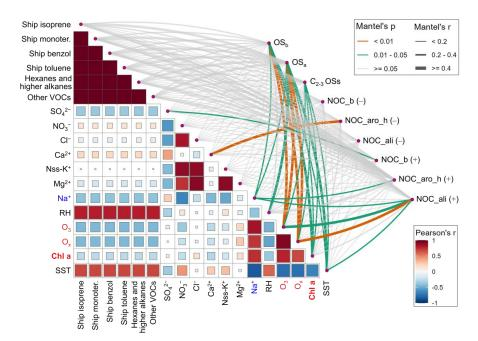


Figure 5. Mantel test correlation heatmap showing the interrelationships between different factors within the same matrix on the left-hand side and the correlation of different matrices on the right-hand side. The size of the solid square indicates the significance of the correlation between the two corresponding parameters. The larger square indicates that the correlation is more significant. The colors of the different solid circles indicate different correlation coefficients (*r*). OS_b comprises OS_i and OS_m. NOC_b incorporates isoprene- and monoterpenes-derived NOCs. NOC_aro_h includes Aro_Re_NOCs, Aro_Ox_NOCs, and heterocyclic-derived NOCs. NOC_ali includes Ali_Re_NOCs and Ali_Ox_NOCs. The '+'and '-' symbols in parentheses refer to the NOCs identified in ESI+ and ESI- modes, respectively.

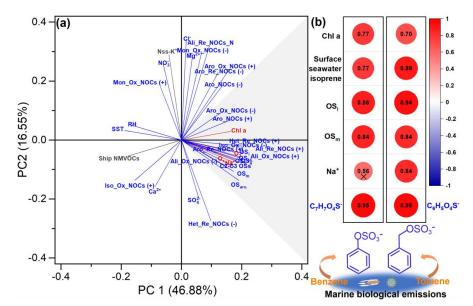


Figure 6. Principal component analysis result (a) deciphering the interrelationships among various OSs, various NOCs, and key factors that likely influence their formation. Diagrams presenting (b) the Spearman correlations between benzene- and toluene-derived OSs and indicators of ocean sources. The colors of the different solid circles indicate different correlation coefficients (r), with specific values labeled directly in the circles. The larger circle indicates that the correlation is more significant, while the symbol "×" indicates that the P value is greater than 0.05. The illustration in the bottom of panel (b) shows that $C_6H_5O_4S^-$ and $C_7H_7O_4S^-$ can be derived from the transformation of marine benzene and toluene.

In addition, we found that aliphatic-, aromatic-, and heterocyclic-derived NOCs identified in ESI+ mode were significantly correlated with either Na⁺ or O₃ and O_x (**Figure 5**). The various NOCs derived from aliphatic, aromatic, and heterocyclic

483

484

485

486

487

488

489

490

491

492

493

494

495

496

497

498

499

500

501

502

503





precursor and the factors including Na⁺, O₃, O_x, and Chl a were also characterized by a high degree of aggregation in the plot of the principal component analysis (Figure 6a). These results provide additional evidence that the abundance of these aromatic and aliphatic NOCs was influenced by marine emissions and atmospheric secondary processes. Aromatic- and heterocyclic-derived NOCs identified in ESI- mode were observed to be closely associated with Ca²⁺ (an indicator of marine source) (Xu et al., 2020a), implying a potential contribution of marine emissions to NOC formation. It is important to acknowledge that the levels of atmospheric NO₂ (5 \pm 6 μg m⁻³) and aerosol NO₃⁻ (0.2 \pm 0.2 μ g m⁻³) and NH₄⁺ (0.7 \pm 0.7 μ g m⁻³) in the Sansha area (Table S1) were considerably lower compared to those observed in urban areas (Xu et al., 2024). The presence of low levels of inorganic nitrogen components posed a substantial restriction on the formation of NOCs. However, these low-level inorganic nitrogen compounds are not the main factors that constrain the formation of OSs. Consequently, the identification of potential sources (primarily marine phytoplankton and other marine biota) contributing to OS formation is indeed indicative of the impact of marine emissions on isoprene-, monoterpenes-, aliphatic-, and aromaticderived SOA in the Sansha area. The release of benzene and toluene from marine organisms has been suggested to be important precursors for marine SOA (Wohl et al., 2023). It has been established that the reaction of benzene and toluene with sulfate radicals in the aqueous phase can lead to the formation of two aromatic OSs, namely C₆H₅O₄S⁻ and C₇H₇O₄S⁻ (Huang et al., 2020). We detected both aromatic OSs in aerosols collected in the Sansha area,





the structures of which were shown in **Figure 6b**. Moreover, we found that these two benzene- and toluene-derived OSs showed significant positive correlations with multiple indicators of marine emissions (e.g., Chl a, surface seawater isoprene, Na⁺, OS_i, and OS_m) (**Figure 6b**). This further corroborates the important effect of marine emissions on the formation of aromatic-derived SOA in the Sansha area.

4. Conclusion and atmospheric implications

Based on our current understanding, this study represents the inaugural instance of simultaneous comprehensive characterization of OSs and NOCs (in both ESI+ and ESI- modes) in PM_{2.5} in tropical marine areas, particularly in Sansha areas with minimal anthropogenic pollution. We concluded that the emissions of marine organisms can contribute to the formation of both typical BSOA (i.e., isoprene and monoterpenes-derived species) and aliphatic- and aromatic-derived SOA in this sea area with few anthropogenic sources of pollution. A recent study in the Yellow Sea of China has reported that marine phytoplankton or microorganisms can contribute to the formation of marine aerosol OS_i and OS_m (Wang et al., 2023). The systematic analysis of this study, including the significant correlation (r = 0.61-0.71, P < 0.01) between estimated surface seawater isoprene and OS_i and OS_m , can indeed directly demonstrate the important role of marine biological emissions in the formation of marine aerosol BSOA. However, the available information regarding the origins of aliphatic and aromatic OSs and NOCs in marine aerosols was previously inadequate. Aerosol aliphatic and aromatic pollutants in marine areas are usually considered to be





transported over long distances from land (Zhou et al., 2023; Sun et al., 2023; Hansen 526 527 et al., 2014). This is the first field observation case to demonstrate that marine organisms can also provide important aliphatic or aromatic precursors for the 528 formation of aliphatic and aromatic OSs and NOCs. 529 530 The presence of benzene and toluene has been observed in the marine and polar atmosphere (Colomb et al., 2009; Wohl et al., 2023). Recent observational evidence 531 532 has indicated that the emission of benzene and toluene from marine organisms 533 contributes to the formation of marine SOA (Wohl et al., 2023). All of these studies 534 underscored the potential of marine organisms to become important contributors to 535 the formation of aliphatic and aromatic OSs and NOCs. If we could directly measure various types of aliphatic and aromatic VOCs on the surface of near sea water in 536 537 remote ocean areas (without human pollution), this would undoubtedly provide the 538 most direct evidence of the aforementioned considerations. However, direct detection is challenging due to the low environmental levels of those VOCs in sea areas with 539 less anthropogenic pollution (lower seawater Chl a levels). Furthermore, low levels of 540 541 marine organisms-derived aliphatic and aromatic VOCs also pose a challenge for 542 directly measuring their characteristic products (e.g., OSs) after oxidation. Thus, the approach of collecting atmospheric fine particles over an extended period (e.g., 23h – 543 168h) (Wang et al., 2023; Hansen et al., 2014; Miyazaki et al., 2016; Lawler et al., 544 545 2020) that we adopt is a highly desirable strategy to maximize the enrichment of SOA components in the sea region. Future studies will necessitate the use of ultra-high 546 resolution mass spectrometry combined with specially designed loading equipment 547





oceans and their fluxes. The generation of SOA on the ocean surface from these 549 550 aliphatic and aromatic precursors also requires systematic mechanistic studies. 551 552 Acknowledgements This study was kindly supported by Key Program of the National Natural Science 553 554 Foundation of China (grant number 42430501), National Natural Science Foundation 555 of China (grant number 42373083), National Key Research and Development Program of China (grant number 2023YFF0806001), and Shanghai "Science and 556 Technology Innovation Action Plan" Shanghai Sailing Program through grant 557 22YF1418700. 558 559 **Conflict of Interest** 560 The authors declare no conflicts of interest relevant to this study. 561 562 563 **Supplementary information** Additional information regarding the descriptions of the sample storage and study site 564 (Text S1 and Figure S1), the analysis and precursor identification of OSs and NOCs 565 (Texts S2-S3, Tables S5-S6, and Figure S2), prediction of pH (Text S4), the OS 566 concentrations showed in previous studies (Table S4), and the data (Tables S1-S3 and 567 568 Figures S3-S5).

for on-line detection of various trace aliphatic and aromatic VOCs released from the





569 References

- 570 Brüggemann, M., Xu, R., Tilgner, A., Kwong, K. C., Mutzel, A., Poon, H. Y.,
- 571 Otto, T., Schaefer, T., Poulain, L., Chan, M. N., and Herrmann, H.: Organosulfates in
- 572 Ambient Aerosol: State of Knowledge and Future Research Directions on Formation,
- 573 Abundance, Fate, and Importance, Environmental Science & Technology, 54, 3767-
- 574 3782, 10.1021/acs.est.9b06751, 2020.
- 575 Bryant, D. J., Elzein, A., Newland, M., White, E., Swift, S., Watkins, A., Deng,
- 576 W., Song, W., Wang, S., Zhang, Y., Wang, X., Rickard, A. R., and Hamilton, J. F.:
- 577 Importance of Oxidants and Temperature in the Formation of Biogenic Organosulfates
- 578 and Nitrooxy Organosulfates, ACS Earth Space Chem., 5, 2291-2306,
- 579 10.1021/acsearthspacechem.1c00204, 2021.
- 580 Budisulistiorini, S. H., Li, X., Bairai, S. T., Renfro, J., Liu, Y., Liu, Y. J.,
- 581 McKinney, K. A., Martin, S. T., McNeill, V. F., Pye, H. O. T., Nenes, A., Neff, M. E.,
- 582 Stone, E. A., Mueller, S., Knote, C., Shaw, S. L., Zhang, Z., Gold, A., and Surratt, J.
- 583 D.: Examining the effects of anthropogenic emissions on isoprene-derived secondary
- 584 organic aerosol formation during the 2013 Southern Oxidant and Aerosol Study
- 585 (SOAS) at the Look Rock, Tennessee ground site, Atmos. Chem. Phys., 15, 8871-
- 586 8888, 10.5194/acp-15-8871-2015, 2015.
- Bushrod, E. E., Thomas, E. R., Zherebker, A., and Giorio, C.: Novel Method to
- 588 Quantify Trace Amounts of Isoprene and Monoterpene Secondary Organic Aerosol-
- 589 Markers in Antarctic Ice, Environmental Science & Technology, 58, 21177-21185,
- 590 10.1021/acs.est.4c09985, 2024.
- 591 Cabrera-Perez, D., Taraborrelli, D., Sander, R., and Pozzer, A.: Global
- 592 atmospheric budget of simple monocyclic aromatic compounds, Atmos. Chem. Phys.,
- 593 16, 6931-6947, 10.5194/acp-16-6931-2016, 2016.
- 594 Carrico, K.: Seeing Sansha: The Political Aesthetics of a South China Sea
- 595 Settlement, Critical Inquiry, 46, 646-664, 10.1086/708070, 2020.
- 596 Chen, H. Y., Chen, L. D., Chiang, Z. Y., Hung, C. C., Lin, F. J., Chou, W. C.,
- 597 Gong, G. C., and Wen, L. S.: Size fractionation and molecular composition of





- 598 water-soluble inorganic and organic nitrogen in aerosols of a coastal environment, J.
- 599 Geophys. Res.: Atmos., 115, doi: 10.1029/2010JD014157., 2010.
- 600 Colomb, A., Gros, V., Alvain, S., Sarda-Esteve, R., Bonsang, B., Moulin, C.,
- 601 Klüpfel, T., and Williams, J.: Variation of atmospheric volatile organic compounds
- 602 over the Southern Indian Ocean (3049S), Environmental Chemistry, 6, 70-82,
- 603 https://doi.org/10.1071/EN08072, 2009.
- 604 Crippa, M., Guizzardi, D., Butler, T., Keating, T., Wu, R., Kaminski, J., Kuenen,
- 605 J., Kurokawa, J., Chatani, S., Morikawa, T., Pouliot, G., Racine, J., Moran, M. D.,
- 606 Klimont, Z., Manseau, P. M., Mashayekhi, R., Henderson, B. H., Smith, S. J., Suchyta,
- 607 H., Muntean, M., Solazzo, E., Banja, M., Schaaf, E., Pagani, F., Woo, J. H., Kim, J.,
- 608 Monforti-Ferrario, F., Pisoni, E., Zhang, J., Niemi, D., Sassi, M., Ansari, T., and Foley,
- 609 K.: The HTAP v3 emission mosaic: merging regional and global monthly emissions
- 610 (2000–2018) to support air quality modelling and policies, Earth Syst. Sci. Data, 15,
- 611 2667-2694, 10.5194/essd-15-2667-2023, 2023.
- Ditto, J. C., Machesky, J., and Gentner, D. R.: Analysis of reduced and oxidized
- 613 nitrogen-containing organic compounds at a coastal site in summer and winter, Atmos.
- 614 Chem. Phys., 22, 3045-3065, 10.5194/acp-22-3045-2022, 2022.
- 615 Gen, M., Huang, D., and Chan, C. K.: Reactive uptake of glyoxal by ammonium
- 616 containing salt particles as a function of relative humidity, Environ. Sci. Technol., 52,
- 617 6903-6911, 2018.
- 618 Guo, Y., Yan, C., Liu, Y., Qiao, X., Zheng, F., Zhang, Y., Zhou, Y., Li, C., Fan, X.,
- 619 Lin, Z., Feng, Z., Zhang, Y., Zheng, P., Tian, L., Nie, W., Wang, Z., Huang, D.,
- 620 Daellenbach, K. R., Yao, L., Dada, L., Bianchi, F., Jiang, J., Liu, Y., Kerminen, V. M.,
- 621 and Kulmala, M.: Seasonal variation in oxygenated organic molecules in urban
- Beijing and their contribution to secondary organic aerosol, Atmos. Chem. Phys., 22,
- 623 10077-10097, 10.5194/acp-22-10077-2022, 2022.
- Hansen, A. M. K., Kristensen, K., Nguyen, Q. T., Zare, A., Cozzi, F., Nøjgaard, J.
- 625 K., Skov, H., Brandt, J., Christensen, J. H., Ström, J., Tunved, P., Krejci, R., and
- 626 Glasius, M.: Organosulfates and organic acids in Arctic aerosols: speciation, annual





- 627 variation and concentration levels, Atmos. Chem. Phys., 14, 7807-7823, 10.5194/acp-
- 628 14-7807-2014, 2014.
- Hawkins, L. N., Russell, L. M., Covert, D. S., Quinn, P. K., and Bates, T. S.:
- 630 Carboxylic acids, sulfates, and organosulfates in processed continental organic aerosol
- 631 over the southeast Pacific Ocean during VOCALS-REx 2008, Journal of Geophysical
- 632 Research: Atmospheres, 115, https://doi.org/10.1029/2009JD013276, 2010.
- 633 Hu, Q.-H., Xie, Z.-Q., Wang, X.-M., Kang, H., He, Q.-F., and Zhang, P.:
- 634 Secondary organic aerosols over oceans via oxidation of isoprene and monoterpenes
- from Arctic to Antarctic, Scientific Reports, 3, 2280, 10.1038/srep02280, 2013.
- Huang, G., Brook, R., Crippa, M., Janssens-Maenhout, G., Schieberle, C., Dore,
- 637 C., Guizzardi, D., Muntean, M., Schaaf, E., and Friedrich, R.: Speciation of
- 638 anthropogenic emissions of non-methane volatile organic compounds: a global
- 639 gridded data set for 1970–2012, Atmos. Chem. Phys., 17, 7683-7701, 10.5194/acp-17-
- 640 7683-2017, 2017.
- Huang, L., Liu, T., and Grassian, V. H.: Radical-Initiated Formation of Aromatic
- 642 Organosulfates and Sulfonates in the Aqueous Phase, Environmental Science &
- 643 Technology, 54, 11857-11864, 10.1021/acs.est.0c05644, 2020.
- Huang, R. J., Zhang, Y., Bozzetti, C., Ho, K. F., Cao, J. J., Han, Y., Daellenbach,
- 645 K. R., Slowik, J. G., Platt, S. M., and Canonaco, F.: High secondary aerosol
- 646 contribution to particulate pollution during haze events in China, Nature, 514, 218-
- 647 222, 2014.
- Jaoui, M., Szmigielski, R., Nestorowicz, K., Kolodziejczyk, A., Sarang, K.,
- 649 Rudzinski, K. J., Konopka, A., Bulska, E., Lewandowski, M., and Kleindienst, T. E.:
- 650 Organic Hydroxy Acids as Highly Oxygenated Molecular (HOM) Tracers for Aged
- 651 Isoprene Aerosol, Environmental Science & Technology, 53, 14516-14527,
- 652 10.1021/acs.est.9b05075, 2019.
- Jimenez, J. L., Canagaratna, M. R., Donahue, N. M., Prevot, A. S. H., Zhang, Q.,
- 654 Kroll, J. H., DeCarlo, P. F., Allan, J. D., Coe, H., Ng, N. L., Aiken, A. C., Docherty, K.
- 655 S., Ulbrich, I. M., Grieshop, A. P., Robinson, A. L., Duplissy, J., Smith, J. D., Wilson,





- 656 K. R., Lanz, V. A., Hueglin, C., Sun, Y. L., Tian, J., Laaksonen, A., Raatikainen, T.,
- 657 Rautiainen, J., Vaattovaara, P., Ehn, M., Kulmala, M., Tomlinson, J. M., Collins, D. R.,
- 658 Cubison, M. J., E., Dunlea, J., Huffman, J. A., Onasch, T. B., Alfarra, M. R., Williams,
- 659 P. I., Bower, K., Kondo, Y., Schneider, J., Drewnick, F., Borrmann, S., Weimer, S.,
- 660 Demerjian, K., Salcedo, D., Cottrell, L., Griffin, R., Takami, A., Miyoshi, T.,
- 661 Hatakeyama, S., Shimono, A., Sun, J. Y., Zhang, Y. M., Dzepina, K., Kimmel, J. R.,
- 662 Sueper, D., Jayne, J. T., Herndon, S. C., Trimborn, A. M., Williams, L. R., Wood, E.
- 663 C., Middlebrook, A. M., Kolb, C. E., Baltensperger, U., and Worsnop, D. R.:
- 664 Evolution of Organic Aerosols in the Atmosphere, Science, 326, 1525-1529,
- doi:10.1126/science.1180353, 2009.
- Kanellopoulos, P. G., Kotsaki, S. P., Chrysochou, E., Koukoulakis, K.,
- 667 Zacharopoulos, N., Philippopoulos, A., and Bakeas, E.: PM2.5-bound organosulfates
- 668 in two Eastern Mediterranean cities: The dominance of isoprene organosulfates,
- 669 Chemosphere, 297, 134103, https://doi.org/10.1016/j.chemosphere.2022.134103,
- 670 2022.
- Lawler, M. J., Lewis, S. L., Russell, L. M., Quinn, P. K., Bates, T. S., Coffman, D.
- 672 J., Upchurch, L. M., and Saltzman, E. S.: North Atlantic marine organic aerosol
- characterized by novel offline thermal desorption mass spectrometry: polysaccharides,
- 674 recalcitrant material, and secondary organics, Atmos. Chem. Phys., 20, 16007-16022,
- 675 10.5194/acp-20-16007-2020, 2020.
- Liang, L., Engling, G., Liu, C., Xu, W., Liu, X., Cheng, Y., Du, Z., Zhang, G.,
- 677 Sun, J., and Zhang, X.: Measurement report: Chemical characteristics of PM2.5
- during typical biomass burning season at an agricultural site of the North China Plain,
- 679 Atmos. Chem. Phys., 21, 3181-3192, 10.5194/acp-21-3181-2021, 2021.
- Ma, Y., Xu, X., Song, W., Geng, F., and Wang, L.: Seasonal and diurnal
- variations of particulate organosulfates in urban Shanghai, China, Atmos. Environ., 85,
- 682 152-160, https://doi.org/10.1016/j.atmosenv.2013.12.017, 2014.
- Ma, Y. J., Xu, Y., Yang, T., Xiao, H. W., and Xiao, H. Y.: Measurement report:
- Characteristics of nitrogen-containing organics in PM2.5 in Ürümqi, northwestern





- 685 China differential impacts of combustion of fresh and aged biomass materials,
- 686 Atmos. Chem. Phys., 24, 4331-4346, 10.5194/acp-24-4331-2024, 2024.
- 687 Ma, Y. J., Xu, Y., Yang, T., Gui, L., Xiao, H. W., Xiao, H., and Xiao, H. Y.: The
- 688 critical role of aqueous-phase processes in aromatic-derived nitrogen-containing
- 689 organic aerosol formation in cities with different energy consumption patterns, Atmos.
- 690 Chem. Phys., 25, 2763-2780, 10.5194/acp-25-2763-2025, 2025.
- 691 Meade, L. E., Riva, M., Blomberg, M. Z., Brock, A. K., Qualters, E. M., Siejack,
- 692 R. A., Ramakrishnan, K., Surratt, J. D., and Kautzman, K. E.: Seasonal variations of
- 693 fine particulate organosulfates derived from biogenic and anthropogenic hydrocarbons
- 694 in the mid-Atlantic United States, Atmospheric Environment, 145, 405-414,
- 695 https://doi.org/10.1016/j.atmosenv.2016.09.028, 2016.
- Meskhidze, N. and Nenes, A.: Phytoplankton and Cloudiness in the Southern
- 697 Ocean, Science, 314, 1419-1423, doi:10.1126/science.1131779, 2006.
- 698 Ming, G.: Assembling a City in the Ocean: Sansha Island in the South China Sea
- 699 and the New Politics of Chinese Territorialization, in: Power Politics in Asia's
- 700 Contested Waters: Territorial Disputes in the South China Sea, edited by: Fels, E., and
- 701 Vu, T.-M., Springer International Publishing, Cham, 225-243, 10.1007/978-3-319-
- 702 26152-2 11, 2016.
- 703 Miyazaki, Y., Coburn, S., Ono, K., Ho, D. T., Pierce, R. B., Kawamura, K., and
- 704 Volkamer, R.: Contribution of dissolved organic matter to submicron water-soluble
- 705 organic aerosols in the marine boundary layer over the eastern equatorial Pacific,
- 706 Atmos. Chem. Phys., 16, 7695-7707, 10.5194/acp-16-7695-2016, 2016.
- Moore, A. N., Cancelada, L., Kimble, K. L. A., and Prather, K. A.: Secondary
- 708 aerosol formation from mixtures of marine volatile organic compounds in a potential
- aerosol mass oxidative flow reactor, Environmental Science: Atmospheres, 4, 351-361,
- 710 10.1039/D3EA00169E, 2024.
- 711 Nie, W., Yan, C., Huang, D. D., Wang, Z., Liu, Y., Qiao, X., Guo, Y., Tian, L.,
- 712 Zheng, P., Xu, Z., Li, Y., Xu, Z., Qi, X., Sun, P., Wang, J., Zheng, F., Li, X., Yin, R.,
- 713 Dallenbach, K. R., Bianchi, F., Petäjä, T., Zhang, Y., Wang, M., Schervish, M., Wang,





- 714 S., Qiao, L., Wang, Q., Zhou, M., Wang, H., Yu, C., Yao, D., Guo, H., Ye, P., Lee, S.,
- 715 Li, Y. J., Liu, Y., Chi, X., Kerminen, V.-M., Ehn, M., Donahue, N. M., Wang, T.,
- 716 Huang, C., Kulmala, M., Worsnop, D., Jiang, J., and Ding, A.: Secondary organic
- 717 aerosol formed by condensing anthropogenic vapours over China's megacities, Nat.
- 718 Geosci., 15, 255-261, 10.1038/s41561-022-00922-5, 2022.
- 719 Riva, M., Chen, Y., Zhang, Y., Lei, Z., Olson, N. E., Boyer, H. C., Narayan, S.,
- 720 Yee, L. D., Green, H. S., Cui, T., Zhang, Z., Baumann, K., Fort, M., Edgerton, E.,
- 721 Budisulistiorini, S. H., Rose, C. A., Ribeiro, I. O., e Oliveira, R. L., dos Santos, E. O.,
- 722 Machado, C. M. D., Szopa, S., Zhao, Y., Alves, E. G., de Sá, S. S., Hu, W., Knipping,
- 723 E. M., Shaw, S. L., Duvoisin Junior, S., de Souza, R. A. F., Palm, B. B., Jimenez, J.-L.,
- 724 Glasius, M., Goldstein, A. H., Pye, H. O. T., Gold, A., Turpin, B. J., Vizuete, W.,
- 725 Martin, S. T., Thornton, J. A., Dutcher, C. S., Ault, A. P., and Surratt, J. D.: Increasing
- 726 Isoprene Epoxydiol-to-Inorganic Sulfate Aerosol Ratio Results in Extensive
- 727 Conversion of Inorganic Sulfate to Organosulfur Forms: Implications for Aerosol
- 728 Physicochemical Properties, Environ. Sci. Technol., 53, 8682-8694,
- 729 10.1021/acs.est.9b01019, 2019.
- 730 Sun, Q., Liang, B., Cai, M., Zhang, Y., Ou, H., Ni, X., Sun, X., Han, B., Deng, X.,
- 731 Zhou, S., and Zhao, J.: Cruise observation of the marine atmosphere and ship
- 732 emissions in South China Sea: Aerosol composition, sources, and the aging process,
- 733 Environmental pollution, 316, 120539, https://doi.org/10.1016/j.envpol.2022.120539,
- 734 2023.
- 735 Surratt, J. D., Gómez-González, Y., Chan, A. W., Vermeylen, R., Shahgholi, M.,
- 736 Kleindienst, T. E., Edney, E. O., Offenberg, J. H., Lewandowski, M., and Jaoui, M.:
- 737 Organosulfate formation in biogenic secondary organic aerosol, J. Phys. Chem. A, 112,
- 738 8345-8378, 2008.
- 739 Takeuchi, M., Berkemeier, T., Eris, G., and Ng, N. L.: Non-linear effects of
- 740 secondary organic aerosol formation and properties in multi-precursor systems,
- 741 Nature Communications, 13, 7883, 10.1038/s41467-022-35546-1, 2022.
- 742 Wang, Y., Zhao, Y., Wang, Y., Yu, J. Z., Shao, J., Liu, P., Zhu, W., Cheng, Z., Li,





- 743 Z., Yan, N., and Xiao, H.: Organosulfates in atmospheric aerosols in Shanghai, China:
- 744 seasonal and interannual variability, origin, and formation mechanisms, Atmos. Chem.
- 745 Phys., 21, 2959-2980, 10.5194/acp-21-2959-2021, 2021.
- 746 Wang, Y., Zhang, Y., Li, W., Wu, G., Qi, Y., Li, S., Zhu, W., Yu, J. Z., Yu, X.,
- 747 Zhang, H.-H., Sun, J., Wang, W., Sheng, L., Yao, X., Gao, H., Huang, C., Ma, Y., and
- 748 Zhou, Y.: Important Roles and Formation of Atmospheric Organosulfates in Marine
- 749 Organic Aerosols: Influence of Phytoplankton Emissions and Anthropogenic
- 750 Pollutants, Environ. Sci. Technol., 57, 10284-10294, 10.1021/acs.est.3c01422, 2023.
- 751 Weisskopf, L., Schulz, S., and Garbeva, P.: Microbial volatile organic
- 752 compounds in intra-kingdom and inter-kingdom interactions, Nature Reviews
- 753 Microbiology, 19, 391-404, 10.1038/s41579-020-00508-1, 2021.
- Wohl, C., Li, Q., Cuevas, C. A., Fernandez, R. P., Yang, M., Saiz-Lopez, A., and
- 755 Simó, R.: Marine biogenic emissions of benzene and toluene and their contribution to
- 756 secondary organic aerosols over the polar oceans, Science Advances, 9, eadd9031,
- 757 doi:10.1126/sciadv.add9031, 2023.
- Wozniak, A. S., Willoughby, A. S., Gurganus, S. C., and Hatcher, P. G.:
- 759 Distinguishing molecular characteristics of aerosol water soluble organic matter from
- 760 the 2011 trans-North Atlantic US GEOTRACES cruise, Atmos. Chem. Phys., 14,
- 761 8419-8434, 10.5194/acp-14-8419-2014, 2014.
- 762 Xiao, H. W., Xiao, H. Y., Luo, L., Shen, C. Y., Long, A. M., Chen, L., Long, Z.
- 763 H., and Li, D. N.: Atmospheric aerosol compositions over the South China Sea:
- temporal variability and source apportionment, Atmos. Chem. Phys., 17, 3199-3214,
- 765 2017.
- 766 Xu, Y., Wu, D. S., Xiao, H. Y., and Zhou, J. X.: Dissolved hydrolyzed amino
- acids in precipitation in suburban Guiyang, southwestern China: Seasonal variations
- 768 and potential atmospheric processes, Atmos. Environ., 211, 247-255.
- 769 https://doi.org/210.1016/j.atmosenv.2019.1005.1011, 2019.
- 770 Xu, Y., Ye, J., Zhou, D., and Su, L.: Research progress on applications of calcium
- 771 derived from marine organisms, Scientific Reports, 10, 18425, 10.1038/s41598-020-





- 772 75575-8, 2020a.
- 773 Xu, Y., Dong, X.-N., Xiao, H.-Y., Zhou, J.-X., and Wu, D.-S.: Proteinaceous
- 774 Matter and Liquid Water in Fine Aerosols in Nanchang, Eastern China: Seasonal
- 775 Variations, Sources, and Potential Connections, J. Geophys. Res.: Atmos., 127,
- e2022JD036589. https://doi.org/036510.031029/032022JD036589, 2022.
- 777 Xu, Y., Dong, X. N., He, C., Wu, D. S., Xiao, H. W., and Xiao, H. Y.: Mist
- 778 cannon trucks can exacerbate the formation of water-soluble organic aerosol and
- 779 PM2.5 pollution in the road environment, Atmos. Chem. Phys., 23, 6775-6788,
- 780 10.5194/acp-23-6775-2023, 2023.
- 781 Xu, Y., Liu, T., Ma, Y. J., Sun, Q. B., Xiao, H. W., Xiao, H., Xiao, H. Y., and Liu,
- 782 C. Q.: Measurement report: Occurrence of aminiums in PM2.5 during winter in China
- 783 aminium outbreak during polluted episodes and potential constraints, Atmos. Chem.
- 784 Phys., 24, 10531-10542, 10.5194/acp-24-10531-2024, 2024.
- Xu, Y., Miyazaki, Y., Tachibana, E., Sato, K., Ramasamy, S., Mochizuki, T.,
- 786 Sadanaga, Y., Nakashima, Y., Sakamoto, Y., Matsuda, K., and Kajii, Y.: Aerosol
- 787 Liquid Water Promotes the Formation of Water-Soluble Organic Nitrogen in
- 788 Submicrometer Aerosols in a Suburban Forest, Environ. Sci. Technol., 54, 1406-1414.
- 789 https://doi.org/1410.1021/acs.est.1409b05849, 2020b.
- 790 Yang, T., Xu, Y., Wang, Y. C., Ma, Y. J., Xiao, H. W., Xiao, H., and Xiao, H. Y.:
- 791 Non-biogenic sources are an important but overlooked contributor to aerosol
- 792 isoprene-derived organosulfates during winter in northern China, Atmos. Chem. Phys.,
- 793 25, 2967-2978, 10.5194/acp-25-2967-2025, 2025.
- 794 Yang, T., Xu, Y., Ma, Y.-J., Wang, Y.-C., Yu, J. Z., Sun, Q.-B., Xiao, H.-W., Xiao,
- 795 H.-Y., and Liu, C.-Q.: Field Evidence for Constraints of Nearly Dry and Weakly
- 796 Acidic Aerosol Conditions on the Formation of Organosulfates, Environ. Sci. Technol.
- 797 Lett., 11, 981-987, 10.1021/acs.estlett.4c00522, 2024.
- 798 Yang, T., Xu, Y., Ye, Q., Ma, Y. J., Wang, Y. C., Yu, J. Z., Duan, Y. S., Li, C. X.,
- 799 Xiao, H. W., Li, Z. Y., Zhao, Y., and Xiao, H. Y.: Spatial and diurnal variations of
- 800 aerosol organosulfates in summertime Shanghai, China: potential influence of





- 801 photochemical processes and anthropogenic sulfate pollution, Atmos. Chem. Phys., 23,
- 802 13433-13450, 10.5194/acp-23-13433-2023, 2023.
- Yu, Z. and Li, Y.: Marine volatile organic compounds and their impacts on
- 804 marine aerosol—A review, Science of The Total Environment, 768, 145054,
- 805 https://doi.org/10.1016/j.scitotenv.2021.145054, 2021.
- Zhai, X., Zhang, H.-H., Yang, G.-P., Li, J.-L., and Yuan, D.: Distribution and sea-
- air fluxes of biogenic gases and relationships with phytoplankton and nutrients in the
- 808 central basin of the South China Sea during summer, Mar. Chem., 200, 33-44,
- 809 https://doi.org/10.1016/j.marchem.2018.01.009, 2018.
- 810 Zhao, D., Yang, Y., Tham, Y. J., and Zou, S.: Emission of marine volatile organic
- 811 compounds (VOCs) by phytoplankton— a review, Marine Environmental Research,
- 812 191, 106177, https://doi.org/10.1016/j.marenvres.2023.106177, 2023.
- Zhou, S., Guo, F., Chao, C.-Y., Yoon, S., Alvarez, S. L., Shrestha, S., Flynn, J. H.,
- 814 III, Usenko, S., Sheesley, R. J., and Griffin, R. J.: Marine Submicron Aerosols from
- 815 the Gulf of Mexico: Polluted and Acidic with Rapid Production of Sulfate and
- 816 Organosulfates, Environmental Science & Technology, 57, 5149-5159,
- 817 10.1021/acs.est.2c05469, 2023.